Journal of Molecular Structure 1291 (2023) 135973

Contents lists available at ScienceDirect

Journal of Molecular Structure

journal homepage: www.elsevier.com/locate/molstr

Cyclocondensation of 3,4-diaminobenzophenone with glyoxal: Synthesis, X-ray structure, density functional theory calculation and molecular docking studies

Yeliz Kaya [a], Savaş Kaya [b], Avni Berisha [c], Ayşe Erçağ [a,*]

[a] Department of Chemistry, Inorganic Chemistry Division, Faculty of Engineering, Istanbul University-Cerrahpaşa, Avcılar, Istanbul 34320, Turkey
[b] Department of Pharmacy, Sivas Cumhuriyet University, Health Services Vocational School, Sivas 58140, Turkey
[c] Department of Chemistry, Faculty of Natural and Mathematics Science, University of Prishtina, Prishtina 10000, Kosovo

ARTICLE INFO

Keywords:
3,4-diaminobenzophenone
Glyoxal
Quinoxaline
DFT
Molecular docking

ABSTRACT

7-benzoyl quinoxaline (BQ) was synthesized by the cyclocondensation of 3,4-diaminobenzophenone with glyoxal. BQ was characterized using elemental analysis (C, H, N), FT-IR, ^{1}H NMR and UV–Visible spectral studies. The crystal structure of BQ was solved by single crystal X-ray diffraction method. Chemical reactivity analysis of the newly synthesized molecule was made with the help of well-known quantum chemical descriptors like hardness, chemical potential, first and second electrophilicity indexes and electronic structure rules like Maximum Hardness Principle of Conceptual Density Functional Theory (CDFT). The results of CDFT based calculations showed that this new molecule is stable and can act a good electron acceptor. Molecular docking studies, providing valuable insights into the biological activity of the novel molecule, highlighted its potential to showcase promising therapeutic characteristics against commonly occurring cancer types. This encouraging behavior will be further validated through upcoming anti-proliferative studies, aiming to confirm its efficacy in combating cancerous cell growth and proliferation.

1. Introduction

Quinoxalines are N-containing heterocyclic compounds of importance in both chemistry and biology. The quinoxaline moiety in a compound serves as the nucleus for the synthesis of biologically active substances. These compounds form the basis of many insecticides, fungicides and herbicides, as well as antitumor, antibacterial, anticancer, anti-inflammatory, antiviral, antimalarial, antibacterial, immunosuppressive/antineoplastic and antidepressant drugs [1–4]. Some antibiotics, such as levomycin, actinoleutin and echinomycin also contain a quinoxaline scaffold and these are found to inhibit the growth of Gram positive bacteria and are active against various transplantable tumors [5,6]. They also find use in dyes, synthesis of organic semiconductors, anion receptors, dehydroannulenes and electrical-photochemical materials [7,8].

After testing the biological activities of quinoxaline compounds, interest in this subject has increased. Many quinoxaline compounds are synthesized and their properties are studied. BQ synthesis using catalysts or different starting materials was given in two separate studies before [7,9]. The substituted quinoxaline derivative derived from phenyl glyoxal and 3,4-diaminobenzophenone was tested in a patented anticarcinogen study [10].

In this context, our interest in quinoxaline chemistry has focused on the synthesis of a quinoxaline derivative, its spectroscopic properties, analysis of its crystal structure, and theoretical (DFT and docking) studies of the molecule.

In this study, BQ was synthesized from the reaction of 3,4-diaminobenzophenone (DAB) with glyoxal in an easy and short-term method without the need for a catalyst. Its structure and spectroscopic properties were tested. By obtaining a single crystal, its three-dimensional crystal structure was resolved by X-ray crystallography and presented here for the first time. Molecular docking studies were performed to determine the possible bioactive properties of the molecule. In addition, density functional theory (DFT) calculations were made and interpreted.

* Corresponding author.
E-mail address: ercaga@iuc.edu.tr (A. Erçağ).

https://doi.org/10.1016/j.molstruc.2023.135973
Received 30 March 2023; Received in revised form 2 June 2023; Accepted 6 June 2023
Available online 7 June 2023

Table 1
Crystal data and structure refinement details.

CCDC	829,160
Empirical formula	$C_{15}H_{10}N_2O$
Formula weight (g.mol^{-1})	234.26
Crystal color, habit	Colorless, chunk
Crystal size (mm)	0.70 × 0.40 × 0.20
Temperature (K)	293.1
Crystal system	Monoclinic
Space group	$P2_1/a$
Cell dimensions	$a = 7.724(5)$ Å $b = 10.4719(4)$ Å $c = 14.5049(8)$ Å $\alpha = 90°$ $\beta = 101.127(3)°$ $\gamma = 90°$
Cell volume (Å^3)	1151.68(11)
Z	4
Density$_{calc}$ (g.cm^{-3})	1.351
μ (mm^{-1})	0.087
F_{000}	488
Index ranges	$-9 \le h \le 8$, $-12 \le k \le 12$, $-17 \le l \le 17$
Reflections collected	44,494
Reflections	2178
Parameters	173
Goodness of fit indicator	0.997
R[$F^2 > 2\sigma(F^2)$]	0.0840
w$R(F^2)$	0.0670
Largest diff. peak and hole (e.Å^{-3})	0.25 and −0.32

2. Experimental

2.1. Materials and methods

3,4-diaminobenzophenone, glyoxal and solvents were used as received from Merck chemical company.

IR spectra were recorded by using an Agilent Cary 630 FTIR-ATR spectrometer. Elemental analyses were carried out on a Thermo Finnigan Flash EA 1112 Series Elemental Analyzer. UV–Vis spectra were recorded in DMF solutions (3×10^{-5}M) on the Shimadzu 2600 UV–Vis Spectrophotometer. ^{1}H NMR spectra were determined by a Varian UNITY INOVA 500 MHz NMR spectrometer using DMSO-d_6 as solvent at room temperature.

2.2. Synthesis

2.2.1. Cyclocondensation of 3,4-diaminobenzophenone with glyoxal

BQ is prepared via a reaction of 3,4-diaminobenzophenone and glyoxal in methanol as shown in Scheme 1. The 3,4-diaminobenzophenone (1 mmol) was dissolved in 5–7 mL methanol with stirring. To this solution, glyoxal (1 mmol) solution was added dropwise. The mixture was heated in a water bath under reflux for 15 min. The reaction was monitored by TLC. After the completion of the reaction, it was left overnight at room temperature. A colorless shiny crystalline solid was obtained. The crystals were washed with cold methanol and vacuum dried. Single crystal suitable for X-ray study was obtained by recrystallization of these crystals in ethanol.

Yield: 98%. Color: Yellow. M.p: 126–127 °C. Calculated for $C_{15}H_{10}N_2O$ (234.25 g mol^{-1}): C 76.91, H 4.30, N 11.96%. Analysis found: C 76.89, H 4.44, N 12.06%. FT-IR (cm^{-1}): υ(CH) 3000–3100, υ(C=O) 1649, υ(C=N) 1607 and 1595. ^{1}H NMR [500 Mhz, DMSO-d_6, δ (ppm)]: 9.05 (dd, 2H, -N=$CH_{(g)}$), 8.31 (d, 1H, -$CH_{(d)}$), 8.26 (d, 1H, -$CH_{(e)}$), 8.17 (dd, 1H, -$CH_{(f)}$), 7.83 (dd, 2H, -$CH_{(a)}$), 7.74 (m, 1H, -$CH_{(c)}$), 7.60 (m, 2H, -$CH_{(b)}$). UV–Vis (DMF) [λ_{max} (nm)]: π→π* 263, π→π* 292, n→π* 320.

2.3. X-Ray crystallography

Suitable single crystals of BQ for X-ray diffraction analysis were obtained by slow evaporation of its ethanol solution at room temperature. The data were collected at a temperature of 20 ± 1 °C to a maximum 2θ value of 50.1°. All measurements were made on a Rigaku R-Axis Rapid-S imaging plate area detector with graphite monochromated Mo-Kα radiation (λ = 0.71070 Å). The crystal structures were solved by SIR 92 [11] and refined with CRYSTALS software package [12]. The non-hydrogen atoms were refined anisotropically. Hydrogen atoms were refined using the riding model. Crystallographic data are given in Table 1. The selected bond distances and bond angles are listed in Table 2.

Table 2
The selected bond lengths (Å) and bond angles (°).

Bond lengths		Bond angles	
C1—O1	1.226(3)	C2—C1—O1	119.5(2)
C13—N2	1.368(3)	C8—C1—O1	120.4(2)
C10—N1	1.366(3)	C10—N1—C11	115.4(2)
C12—N2	1.292(4)	C13—N2—C12	116.1(2)
C11—N1	1.307(3)	C2—C1—C8	120.1(2)

2.4. Conceptual density functional theory (CDFT) based calculations

The prediction of chemical reactivity of the chemical systems via simple and useful equations is among the facilities provided via Conceptual DFT to theoretical chemists and physicists. In this theory, starting from the relationship between total electronic energy (E) and the total number of electrons (N) for any chemical systems, important equations to compute the parameters such as chemical potential (μ), electronegativity (χ), hardness (η) and softness (σ) have been derived. CDFT presents the following mathematical models for chemical potential and chemical hardness, respectively [13–15].

$$\mu = \left[\frac{\partial E}{\partial N}\right]_{\nu(r)}$$

$$\eta = \left[\frac{\partial \mu}{\partial N}\right]_{\nu(r)} = \left[\frac{\partial^2 E}{\partial N^2}\right]_{\nu(r)}$$

Electronegativity is given the negative of the chemical potential while softness is mathematically presented as the multiplicative inverse of hardness.

$$\chi = -\mu$$

$$\sigma = 1/\eta$$

Applying the finite differences approach to the mathematical relations given above, one can get the following equations to compute these quantum chemical parameters [16,17].

$$\mu = -\chi = -\left(\frac{I + A}{2}\right)$$

$$\eta = I - A$$

$$\sigma = 1/(I - A)$$

Here, I and A are ionization energy and electron affinity, respectively. In especially organic chemistry, electrophilicity and nucleophilicity concepts are widely considered in the studies regarding to the reaction mechanisms and chemical binding. One of the main goals of theoretical chemists is to derive the simple and useful formula to compute such well-known parameters. In 1999, as a result of a range of logical approaches; Parr, Szentpaly and Liu introduced the electrophilicity index (ω) as [18]:

$$\omega = \chi^2/2\eta = \mu^2/2\eta$$

The second electrophilicity index (ω_2) whose usefulness and validity

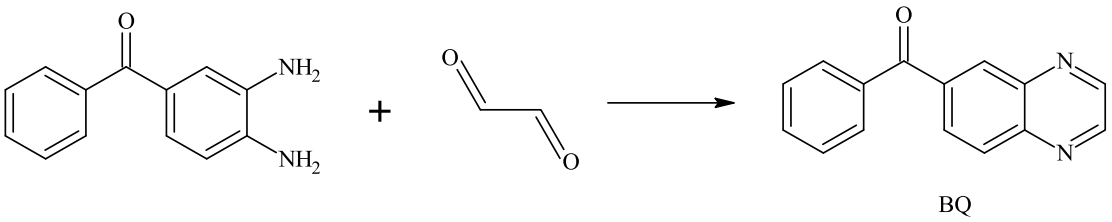

Scheme 1. Synthesis of BQ.

are supported by Szentpály and Kaya [19] based on the valence state parabola model is calculated from the following formula:

$$\omega_2 = \frac{I.A}{I-A}$$

To predict the electron transfer between chemical systems and to highlight the nature of the chemical interactions, theoretical chemists continue to add new parameters to CDFT. The electron donating power (ω^-) and electron accepting power (ω^+) parameters introduced by Gazquez and coworkers [20] are calculated as:

$$\omega^- = (3I+A)^2/(16(I-A))$$

$$\omega^+ = (I+3A)^2/(16(I-A))$$

In the present study, the chemical reactivity of the synthesized molecule by us was analyzed in the light of the CDFT based quantum chemical parameters. The ionization energy and electron affinity of this molecule were predicted via Koopmans Theorem [21] presenting the following relations:

$$I = -E_{HOMO}$$

$$A = -E_{LUMO}$$

2.5. Molecular docking and molecular mechanics (MM) studies

The docking interactions were investigated using Maestro (Schrödinger Inc.). The analysis was carried out to determine the potential binding interactions of the chosen ligand with the receptor's active site. Maestro's LigPrep module was used to prepare the ligand structure. Ligands were aided in binding in more than one potential conformation by grid-based molecular docking. The protein structure was created in Maestro using the protein preparation wizard (preprocessed, optimized, and minimized). To match a pH of 7.4, the protonation and tautomeric states of amino acids were modified. Maestro's receptor grid creation module was used to generate the grid; 0.25, scaling factor, and 1.0, partial charge cut off for van der Waals radius were used. Docking was done in XP (extra precision) mode. Glide molecular docking was used to assess binding interactions and ligand flexibility. Binding energies in kcal/mol were computed. The XP Visualizer was used to examine the individual ligand-protein interactions. The protein with the pdb id: 4HJO was obtained from the Protein Data Bank [22]. After drawing the structure of the ligand via Avogadro software the structure was optimized and saved as a .sdf file [23].

Afterward to obtain the lowest energy structure and flexibility of study of the molecule (an important factor in docking studies) [24] both DFT and Molecular Mechanics (MM) calculations were performed. The DFT results were acquired via the following level of theory: m-GGA/M06L [25,26] /DNP [27] /COMSO [28–30] (solvent: methanol), whereas for MM conformer search the following conditions for the calculations were applied: Search method → Random sampling; Number of conformers → 500; Torsion angle window → 10; Forcefield: COMPASS III [31].

3. Result and discussion

3.1. Synthesis and spectroscopy

BQ was prepared by the cyclocondensation of 3,4-diaminobenzophenone (1 mmol) with glyoxal (1 mmol) (Scheme 1). BQ is soluble in methanol, ethanol, THF, DCM, DMF, DMSO, chloroform, acetonitrile, toluene and 1,4-dioxane solvents. The elemental analysis and spectroscopic data agreed with the proposed molecular formula of BQ.

The typical stretching band at 1660 cm^{-1} belonging to the C=O group of 3,4-diaminobenzophenone was examined at 1649 cm^{-1} with a slight shift in the IR spectrum of BQ. In the spectrum of BQ, bands in the range of 3429–3281 cm^{-1}, which are assigned to the asymmetric and symmetric stretching modes of N-H in the amine groups of 3,4-diaminobenzophenone, are not seen. In addition, new C=N bands, which are formed as a result of the cyclocondensation of glyoxal with

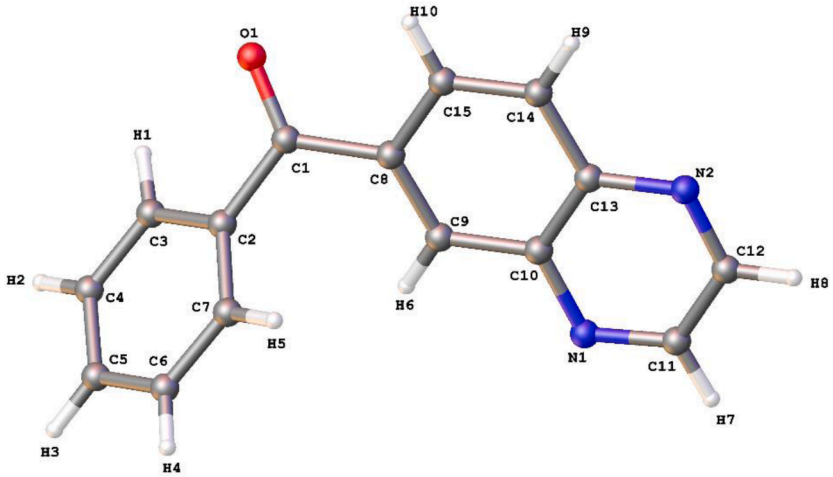

Fig. 1. Molecular structure of BQ with the atom numbering scheme.

Table 3
Calculated CDFT based parameters for the synthesized molecule.

E_{HOMO}	−6.280 eV
E_{LUMO}	−3.206 eV
I	6.280 eV
A	3.206 eV
μ	−4.743
χ	4.743
η	3.074
ω	3.659
ω_2	6.549
ω^-	9.881
ω^+	5.138

benzophenone, are seen at 1607 cm^{-1} and 1595 cm^{-1} in the spectrum of BQ [32–34]. IR spectra of 3,4-diaminobenzophenone and BQ are given in Figs. S1 and S2.

Peaks belonging to -NH_2 groups at 3.31 ppm and 3.83 ppm in the ^1H NMR spectrum of 3,4-diaminobenzophenone are not observed in the spectrum of BQ. The newly formed CH=N peaks as a result of cyclo-condensation are also seen at 9.05 ppm. These results show the formation of quinoxaline. Also, the multiplets of the aromatic protons of BQ appear within the range 7.60–8.31 ppm [9]. ^1H NMR spectra of 3,4-diaminobenzophenone and BQ are given in Figs. S3–S5.

The UV–Vis absorption spectrum of BQ shows bands at 263 and 320 (shoulder) nm. The bands at 263 nm can be attributed to the π–π* transition of the benzene rings. The absorption band at around 320 nm is due to n–π* transitions of the C=N chromophore groups [34,35]. UV–Vis spectra of 3,4-diaminobenzophenone and BQ are given in Figs. S6 and S7.

3.2. Crystallographic descriptions

Slow evaporation of BQ in ethanol gave crystals suitable for X-ray crystallography analysis. The compound crystallizes in the monoclinic space group $P2_1/a$ with $a = 7.724(5)$ Å, $b = 10.4719(4)$ Å, $c = 14.5049(8)$ Å, $\alpha = 90°$, $\beta = 101.127(3)°$, $\gamma = 90°$ and $Z = 4$. The molecular structure of BQ with the atom numbering scheme is shown in Fig. 1. Crystal data and structure refinement are tabulated in Table 1. The C1=O1 double bond distance [1.226(3) Å] is close to the distances obtained in similar structures [33,36–38]. The C13-N2 [1.368(3) Å], C10-N1 [1.366(3) Å], C12-N2 [1.292(4) Å] and C11-N1 [1.307(3) Å] bond distances in the molecule are intermediate between 1.43 and 1.45 Å for an ideal C-N single bond and 1.28 Å for an ideal C=N double bond, indicating of electron delocalization in the molecule [32,38] (Table 2).

3.3. DFT studies

In Table 3, calculated quantum chemical parameters for our new molecules are given. Fig. 2 visually presents the optimized structure, HOMO, LUMO and ESP images of the synthesized molecule. Red region appearing in ESP map is the region where the negative charge is concentrated. This molecule interacts with metal surfaces and metal cations via this region. Frontier orbital energies provide a useful strategy to predict the electron donating and electron accepting capabilities of molecules. It should be noted that the chemical systems with high E_{HOMO} values are good electron donors while the molecules with low E_{LUMO} values act as good electron acceptors. Chemical hardness [39–41] is the resistance exhibited against the polarization of the electron cloud of atoms, ions and molecules. Hard and Soft Acid Base (HSAB) Principle [42] includes the classification of Lewis acids and bases as hard and soft. In this classification, it is seen that hard molecules exhibit high resistance against polarization while soft molecules have high polarization. Maximum Hardness Rule [43] states that "It seems to be a rule of nature that molecules arrange themselves so as to be as hard as possible". From this explanation, it can be easily deduced that chemical hardness is an indicator of stability and hard chemical systems are more stable compared to soft molecules. Calculated chemical hardness value for our molecule is 3.074 eV. There is proportionality between hardness and electronegativity as noted by Bratsch. Electronegativity is the electron withdrawal power of atoms and molecules. Electronegativity value calculated for our molecule is 4.743 eV. Looking at the calculated hardness and electronegativity values, it can be said that our synthesized molecule is stable. Electron accepting power and electrophilicity index values also imply that this molecule highly tends to attract electrons. Conceptual Density Functional parameters calculated will be useful in the design and synthesis of such type molecules in future experimental studies.

Density Functional Theory plays a significant role in drug discovery and development by providing computational tools to investigate the

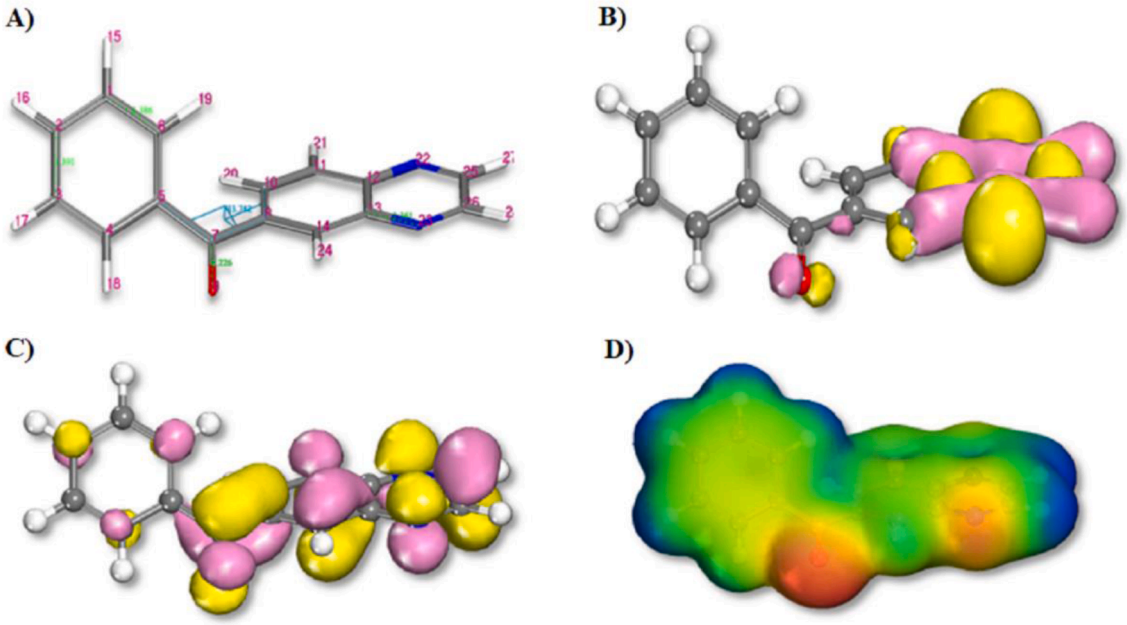

Fig. 2. (. A) Optimized structure, (B) HOMO, (C) LUMO and (D) ESP images of the synthesized molecule.

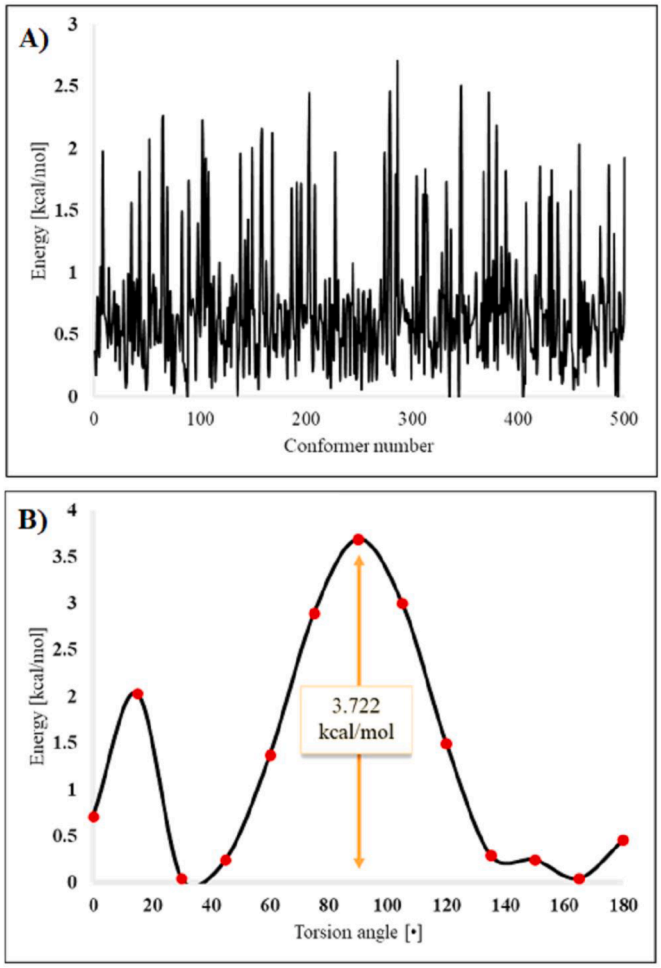

Fig. 3. (. A) Conformer research and (B) Rotation barrier of the studied molecule.

electronic structure, reactivity, binding affinity, and other relevant properties of drug molecules. These insights can guide the design and optimization of novel drugs with improved efficacy, selectivity, and pharmacokinetic properties. The computation of Electrostatic Potential (ESP) using Density Functional Theory (DFT) in drug discovery and development might provide useful insights into the electrostatic characteristics of therapeutic compounds and their interactions with biological targets. Furthermore, ESP gives portions of the drug molecule that may create favorable interactions with the target receptor, such as hydrogen bonding or ion-dipole interactions, by studying the distribution of charges. This data can be used to better understand the molecule's overall charge distribution and its ability to interact with charged areas of the target protein or receptor, but also solvation properties of the drug. ESP calculations are frequently integrated with other computational methods and experimental data to provide a full knowledge of drug compounds' molecular characteristics and behavior. As displayed in Fig. 2, the molecule has both hydrophilic (red regions) and hydrophobic (blue regions) components that give a means to interact with and exhibit pharmacological behavior with the protein structure.

3.4. Docking studies

As seen in Fig. 3, the rotation barrier for the molecule is quite low and is comparable to other molecules possessing this single bond rotation [44], meaning that the molecule is flexible and can adopt easily to the shape of the protein pocket.

The epidermal growth factor receptor (EGFR), a cell-surface receptor for epidermal growth factor members, was chosen as the study's target [45]. The EGFR is required for mammary gland ductal development, and when the protein is overexpressed, it causes a variety of malignancies, including epithelial tumors of the head and neck and anal cancers [46]. In Figs. 4, 2D and 3D structures regarding to the interaction with EGFR of our designed molecule are given. According to the docking profile, the ligand had a defined and strong binding affinity for the epidermal growth factor receptor, as evidenced by the docking score values. Standard inhibitor binds to the target site of the following protein side chains by several pi-alkyl bonding interactions with: LEU 753, LYS 721, VAL 702, and ALA 719; van der Waals bonding interaction with: PHE 832, CYS 751, THR 766, ASP 831, THR 830, and ILE 720; and pi-sulfur bonding interaction with MET 742 and a docking score of −6.19 with an dG binding value of −39.91 kcal/mol (evaluated via: Molecular mechanics with generalized Born and surface area solvation: MM-GBSA scheme) [47]. Both, docking score and dG values are indicative of the strong affinity of this ligand toward the EGFR.

4. Conclusion

Our work is based on the cyclodensation of 1,2-diamino compound, 3,4-diaminobenzophenone and 1,2-dicarbonyl compound glyoxal. As a result, the synthesis of quinoxaline as described herein is simple and extremely rapid. It also provides high (almost quantitative) yields. It can be seen from the calculated CDFT based chemical reactivity descriptors

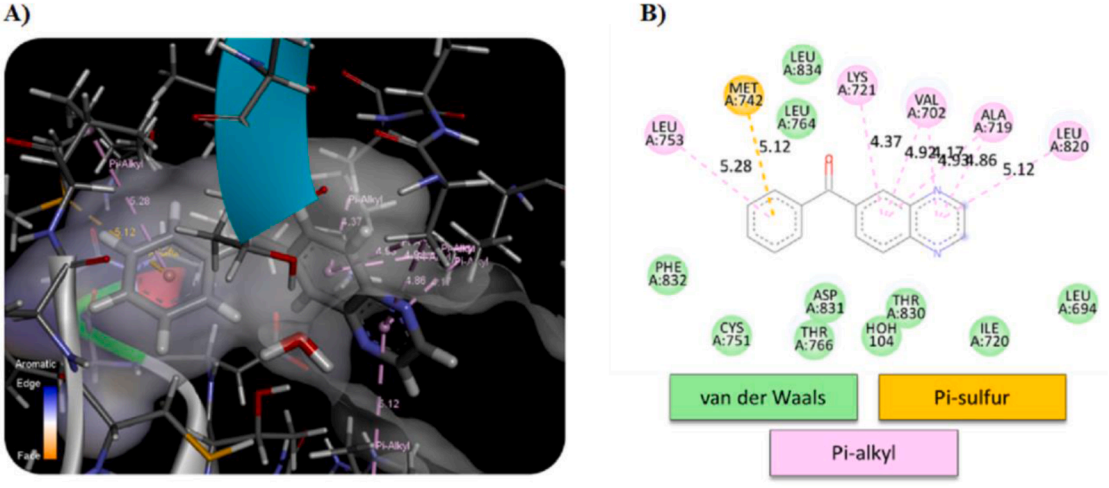

Fig. 4. The interaction with selected molecular system (EGFR) (A: 3D and B: 2D images).

that the compound (BQ) exhibit high stability and can act a good electron acceptor. Through the molecular docking analysis, it was noted that this molecule can powerfully interact with some biological systems and can be considered in future drug design studies focusing on some common cancer types.

Funding

This work was supported by the Scientific Research Projects Coordination Unit of Istanbul University-Cerrahpaşa (Project Number FYL-2016-20292).

CRediT authorship contribution statement

Yeliz Kaya: Data curation, Investigation, Visualization, Writing – review & editing. **Savaş Kaya:** Data curation, Software, Visualization, Writing – review & editing. **Avni Berisha:** Data curation, Software, Visualization, Writing – review & editing. **Ayşe Erçağ:** Conceptualization, Project administration, Supervision, Writing – original draft, Writing – review & editing.

Declaration of Competing Interest

The authors declare that they have no conflicts of interest.

Data availability

No data was used for the research described in the article.

Acknowledgment

We are thankful to Prof. Dr. Yunus ZORLU for his assistance in interpreting the X-ray crystallographic study data. We are also thankful to Sevinç Aydınlar and Tuba Kuş for their assistance in the synthesis studies.

Supplementary materials

Supplementary material associated with this article can be found, in the online version, at doi:10.1016/j.molstruc.2023.135973.

References

[1] S.B. Wadavrao, R.S. Ghogare, A.V. Narsaiah, A simple and efficient protocol for the synthesis of quinoxalines catalyzed by pyridine, Org. Commun. 6 (2013) 23–30.
[2] A.A. Abu-Hashem, Synthesis, reactions and biological activity of quinoxaline derivatives, Am. J. Org. Chem. 5 (2015) 14–56.
[3] H. Khatoon, E. Abdulmalek, Novel synthetic routes to prepare biologically active quinoxalines and their derivatives: A synthetic review for the last two decades, Molecules 26 (2021) 1055.
[4] E. Ghobadi, M. Peiravi, E. Kolvari, Green SDS-assisted synthesis of quinoxaline derivatives in the water, J. Appl. Chem. 10 (2016) 49–54.
[5] D. Bandyopadhyay, S. Mukherjee, R.R. Rodriguez, B.K. Banik, An effective microwave-induced iodine-catalyzed method for the synthesis of quinoxalines via condensation of 1,2-diamines with 1,2-dicarbonyl compounds, Molecules 15 (2010) 4207–4212.
[6] M.A. El-Atawy, E.A. Hamed, M. Alhadi, A.Z. Omar, Synthesis and antimicrobial activity of some new substituted quinoxalines, Molecules 24 (2019) 4198.
[7] B. Karami, S. Khodabakhshi, A novel and simple synthesis of some new and known dibenzo phenazine and quinoxaline derivatives using lead dichloride, J. Chil. Chem. Soc. 58 (2013) 1655–1658.
[8] V. Elumalai, J.H. Hansen, A green, scalable, and catalyst-free one-minute synthesis of quinoxalines, SynOpen 5 (2021) 43–48.
[9] H. Neumann, A. Brennführer, M. Beller, A general synthesis of diarylketones by means of a three-component cross-coupling of aryl and heteroaryl bromides, carbon monoxide, and boronic acids, Chem. Eur. J. 14 (2008) 3645–3652.
[10] K.P. Hirth, E. Mann, L.K. Shawyer, A. Ullrich, I. Szekely, T. Bajor, J. Haimichael, L. Orfi, A. Levitzki, A. Gazit, P.C. Tang, R. Lammers, Treatment of platelet derived growth factor related disorders such as cancers, University of California, Yissum Research Development Company of the Hebrew University of Jerusalem, Biosignal LTD, Sugen, Inc., Max-Planck-Gesellschaft Zur Forderung der Wissenschaften E.V., United States, 2001, pp. 1–82.
[11] A. Altomare, G. Cascarano, C. Giacovazzo, A. Guagliardi, M.C. Burla, G. Polidori, M. Camalli, *SIRPOW*.92 – a program for automatic solution of crystal structures by direct methods optimized for powder data, J. Appl. Crystallogr. 27 (1994) 435–436.
[12] D.J. Watkin, C.K. Prout, J.R. Carruthers, P.W. Betteridge, CRYSTALS Issue 10, Chemical Crystallography Laboratory, University of Oxford, Oxford, 1996, pp. 1–23.
[13] N. Islam, S. Kaya, Conceptual density functional theory and its application in the chemical domain, CRC Press, New Jersey, 2018.
[14] Ş. Berk, S. Kaya, E.K. Akkol, H. Bardakçı, A comprehensive and current review on the role of flavonoids in lung cancer: Experimental and theoretical approaches, Phytomedicine 98 (2022), 153938.
[15] G. Serdaroğlu, S. Kaya, R. Touir, Eco-friendly sodium gluconate and trisodium citrate inhibitors for low carbon steel in simulated cooling water system: Theoretical study and molecular dynamic simulations, J. Mol. Liq. 319 (2020), 114108.
[16] Y. El aoufir, S. Zehra, H. Lgaz, A. Chaouiki, H. Serrar, S. Kaya, R. Salghi, S. K. AbdelRaheem, S. Boukhris, A. Guenbour, I.-M. Chung, Evaluation of inhibitive and adsorption behavior of thiazole-4-carboxylates on mild steel corrosion in HCl, Colloids Surf. A: Physicochem. Eng. Asp. 606 (2020), 125351.
[17] L. Guo, Z.S. Safi, S. Kaya, W. Shi, B. Tüzün, N. Altunay, C. Kaya, Anticorrosive effects of some thiophene derivatives against the corrosion of iron: a computational study, Front. Chem. 6 (2018) 155.
[18] R.G. Parr, L. von Szentpály, S. Liu, Electrophilicity index, J. Am. Chem. Soc. 121 (1999) 1922–1924.
[19] L.s.von Szentpály, S. Kaya, N. Karakuş, Why and when is electrophilicity minimized? New theorems and guiding rules, The J. Phys. Chem. A 124 (2020) 10897–10908.
[20] J.L. Gázquez, A. Cedillo, A. Vela, Electrodonating and electroaccepting powers, The J. Phys. Chem. A. 111 (2007) 1966–1970.
[21] T. Koopmans, Über die Zuordnung von Wellenfunktionen und Eigenwerten zu den Einzelnen Elektronen Eines Atoms, Physica 1 (1934) 104–113.
[22] H. Berman, K. Henrick, H. Nakamura, Announcing the worldwide protein data bank, Nat. Struct. Mol. Biol. 10 (2003).980-980.
[23] M.D. Hanwell, D.E. Curtis, D.C. Lonie, T. Vandermeersch, E. Zurek, G.R. Hutchison, Avogadro: an advanced semantic chemical editor, visualization, and analysis platform, J. Cheminf. 4 (2012) 1–17.
[24] S.-Y. Huang, Comprehensive assessment of flexible-ligand docking algorithms: current effectiveness and challenges, Briefings Bioinf 19 (2018) 982–994.
[25] Y. Zhao, D.G. Truhlar, The M06 suite of density functionals for main group thermochemistry, thermochemical kinetics, noncovalent interactions, excited states, and transition elements: two new functionals and systematic testing of four M06-class functionals and 12 other functionals, Theor. Chem. Acc. 120 (2008) 215–241.
[26] S.E. Wheeler, K.N. Houk, Integration grid errors for meta-GGA-predicted reaction energies: Origin of grid errors for the M06 suite of functionals, J. Chem. Theory Comput. 6 (2010) 395–404.
[27] Y. Inada, H. Orita, Efficiency of numerical basis sets for predicting the binding energies of hydrogen bonded complexes: Evidence of small basis set superposition error compared to Gaussian basis sets, J. Comput. Chem. 29 (2008) 225–232.
[28] A. Klamt, The COSMO and COSMO-RS solvation models, WIREs Comput. Mol. Sci. 8 (2018) e1338.
[29] A. Berisha, Interactions between the aryldiazonium cations and graphene oxide: A DFT study, J. Chem. 2019 (2019) 1–5.
[30] A. Klamt, COSMO-RS: From quantum chemistry to fluid phase thermodynamics and drug design, Elsevier, Amsterdam, 2005.
[31] R.L.C. Akkermans, N.A. Spenley, S.H. Robertson, COMPASS III: Automated fitting workflows and extension to ionic liquids, Mol. Simul. 47 (2021) 540–551.
[32] T. Ben Rhaiem, H. Boughzala, A. Driss, Synthesis, crystal structure, and comparative study of a new organic material 3,4-diaminobenzophenone semihydrate, J. Chem. 2013 (2013) 1–7.
[33] E. Dilmen Portakal, Y. Kaya, E. Demirayak, E. Karacan Yeldir, A. Erçağ, İ. Kaya, Ni (II), Zn(II), and Fe(III) complexes derived from novel unsymmetrical salen-type ligands: preparation, characterization and some properties, J. Coord. Chem. 75 (2022) 611–628.
[34] E. Dilmen Portakal, Y. Kaya, E. Demirayak, E. Karacan Yeldir, A. Erçağ, İ. Kaya, Synthesis, characterization, and investigation of some properties of the new symmetrical bisimine Ni(II), Zn(II), and Fe(III) complexes derived from the monoimine ligand, Appl. Organomet. Chem. 35 (2021) e6265.
[35] H. Bahron, S.S. Khaidir, A.M. Tajuddin, K. Ramasamy, B.M. Yamin, Synthesis, characterization and anticancer activity of mono- and dinuclear Ni(II) and Co(II) complexes of a Schiff base derived from *o*-vanillin, Polyhedron 161 (2019) 84–92.
[36] E.B. Fleischer, N. Sung, S. Hawkinson, Crystal structure of benzophenone, The J. Phys. Chem. 72 (1968) 4311–4312.
[37] L. Antolini, I.M. Vezzosi, L.P. Battaglia, A.B. Corradi, Crystal and molecular structures of 2-aminobenzophenone and 2-aminodiphenylmethanol, J. Chem. Soc., Perkin Trans. 2. (1985) 237–239.
[38] F.H. Allen, O. Kennard, D.G. Watson, L. Brammer, A.G. Orpen, R. Taylor, Tables of bond lengths determined by X-ray and neutron diffraction. Part 1. Bond lengths in organic compounds, J. Chem. Soc., Perkin Trans. 2. (1987) S1–S19.
[39] S. Kaya, C. Kaya, A new equation for calculation of chemical hardness of groups and molecules, Mol. Phys. 113 (2015) 1311–1319.
[40] S. Kaya, C. Kaya, A new method for calculation of molecular hardness: A theoretical study, Comput. Theor. Chem. 1060 (2015) 66–70.

[41] S. Kaya, C. Kaya, A simple method for the calculation of lattice energies of inorganic ionic crystals based on the chemical hardness, Inorg. Chem. 54 (2015) 8207–8213.
[42] R.G. Pearson, Hard and soft acids and bases, J. Am. Chem. Soc. 85 (1963) 3533–3539.
[43] S. Kaya, C. Kaya, N. Islam, Maximum hardness and minimum polarizability principles through lattice energies of ionic compounds, Phys. B. 485 (2016) 60–66.
[44] R.F. Quijano-Quiñones, M. Quesadas-Rojas, G. Cuevas, G.J. Mena-Rejón, The rotational barrier in ethane: A molecular orbital study, Molecules 17 (2012) 4661–4671.
[45] S. Kethireddy, S. Ketha, L. Eppakayala, S. Chithaluri, Anti-cancer docking investigations of Quinoxaline phenyl thiazolidinones, Vietnam J. Chem. 60 (2022) 346–353.
[46] R. Roskoski Jr, The ErbB/HER family of protein-tyrosine kinases and cancer, Pharmacol. Res. 79 (2014) 34–74.
[47] S. Genheden, U. Ryde, The MM/PBSA and MM/GBSA methods to estimate ligand-binding affinities, Expert Opin. Drug Discovery. 10 (2015) 449–461.